Plasmonics
DOI 10.1007/s11468-016-0228-z

Ultra-Subwavelength and Low Loss in V-Shaped Hybrid Plasmonic Waveguide

Yongyuan Zhang [1,2] · **Zhongyue Zhang** [1]

Received: 3 November 2015 / Accepted: 28 March 2016

Abstract A new kind of hybrid plasmonic waveguide is proposed, and its propagation properties are investigated using the finite-element method. This waveguide consists of a V-shaped silver nanowire embedded in a low-index dielectric cladding above a semiconductor substrate, which can confine light in the subwavelength region with a long propagation length. The field distribution, the mode effective index, the propagation length, and the normalized mode area of the hybrid mode supported by the waveguide are investigated at the wavelength of 1550 nm, which are dependent on the geometric parameters.

Keywords Surface plasmon polaritons · Waveguides · Subwavelength nanophotonic integrated circuits

Introduction

Surface plasmon polaritons (SPPs) are electromagnetic waves that propagate along the interface between a metal and a dielectric with their power exponentially decaying in both media [1]. SPPs waveguides are regarded as the suitable candidates for guiding light in nanophotonic integrated circuits due to they can confine and guide light in nanoscale beyond the diffraction limit [2, 3]. Till now, a variety of plasmonic structures have been demonstrated numerically and experimentally, such as metal nanowire waveguides [4–7], metal slot waveguides [8–10], metal-insulator-metal waveguides [11, 12], and metal wedge waveguides [13–16]. However, due to the large ohmic loss induced by the metallic components, there is a trade-off relation between the field confinement and propagation length for these plasmonic waveguides. In general, a good field confinement is usually accompanied with a very short propagation length and vice versa.

In order to balance the trade-off relation between the field confinement and propagation length, a so-called hybrid plasmonic waveguide (HPW) has been proposed [17, 18]. Recently a number of HPW consisting of a metallic nanostructure embedded in a low-index dielectric cladding above a high-index substrate have been proposed and demonstrated [19–34], which showed that a strong confinement with reasonable propagation length could be gained. In order to improve the density of the circuit and components in subwavelength photonic integrations, it is hoped that the field confinement is stronger the better. Researches show that the narrow space between the metal and dielectric can confine light; on the other hand, sharp metallic edges have good field confinement [35].

In this paper, combining a low-index dielectric nanoscale gap and sharp metallic edges, we propose a new kind of HPW, which consists of a V-shaped silver nanowire embedded in a low-index dielectric cladding above a semiconductor substrate. Numerical simulation results show that the proposed HPW could achieve very small effective mode area and long propagation length. Our analysis revealed that the mechanisms of the strong field confinement are the lateral confinement and field enhancement around the tip of V-shaped silver nanowire.

✉ Zhongyue Zhang
zyzhang@snnu.edu.cn

[1] School of Physics and Information Technology, Shaanxi Normal University, Xi'an 710062, China

[2] School of Science, Xi'an University of Science and Technology, Xi'an 710054, China

Published online: 08 April 2016

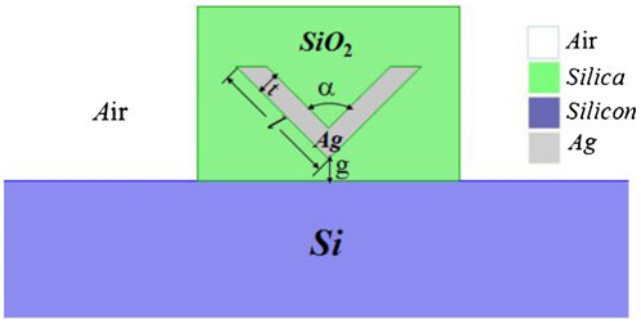

Fig. 1 Schematic diagram of the cross-section of the proposed HPW

Waveguide Structure

The cross section schematic geometry of proposed V-Shaped HPW is shown in Fig. 1, where a V-shaped silver nanowire is separated from the semiconductor (Si) substrate by a nanoscale low-index dielectric (SiO_2) gap with height of g. The hypotenuse, thickness, and vertex angle of the V-shaped silver wedge are denoted as l, t, and α, respectively. The length and width of the dielectric (SiO_2) are 800 and 600 nm, respectively. The characteristics of the V-shaped HPW are investigated at the telecommunication wavelength $\lambda = 1550$ nm, and the refractive index of silver is obtained from Ref. [36]. The refractive indices of Si and SiO_2 are set to 3.476 and 1.444, respectively.

The characteristics of the studied waveguide are investigated using the RF module of the finite-element-based software Comsol Multiphysics 4.3. The main properties of plasmonic waveguides include the mode effective index (N_{eff}), the propagation length (L_m), and the normalized mode area (A_{eff}/A_0). Here N_{eff} is defined as k/k_0, where k and $k_0 = 2\pi/\lambda$ are the propagation constants of the SPPs and the free space wave number, respectively. The propagation length is defined as the distance at which the field amplitude drops to 1/e of its initial value and calculated as $L_m = \lambda/[4\pi \mathrm{Im}(N_{eff})]$, where $\mathrm{Im}(N_{eff})$ is the imaginary part of N_{eff}. The normalized mode area is expressed by the formula A_{eff}/A_0, where $A_0 = \lambda^2/4$ is the diffraction-limited mode area in free space and the effective mode area A_{eff} is defined as:

$$A_{eff} = \iint W(x,y)dxdy/\max[W(x,y)]$$

Where $W(x,y) = \frac{1}{2}\varepsilon|E|^2 + \frac{1}{2}\mu_0|H|^2$ is the energy density and E, H, ε, μ_0 being the electric field, magnetic field, dielectric permittivity, and vacuum magnetic permeability, respectively.

Numerical Results and Discussions

For comparison with the proposed hybrid waveguide, a V-shaped silver nanowire embedded in air and a V-shaped silver nanowire embedded in air clading above Si substrate are also investigated at the telecommunication wavelength $\lambda = 1550$ nm, where the hypotenuse, thickness and the vertex angle of the V-shaped silver wedge are fixed at 300 nm, 50 nm, and 90°, respectively. The electric field patterns of the three waveguides are shown in Fig. 2a–c. As shown in Fig. 2a, the light is distributed in three tips of the V-shaped silver nanowire from Fig. 2b, c, it is clear that the light is tightly confined in the nanoscale gap; it makes light propagation in the non-metallic regions, thus enabling strong confinement with reasonable propagation length. The normalized mode areas of the structures in Fig. 2a–c are 0.00253, 0.00704, and 0.00235 with the propagation lengths are 69.8, 1260.4, and 220.8 μm, respectively. Therefore, the proposed hybrid waveguide shows great advantages of better confinement with moderate propagation length.

The dimensions of the V-shaped silver strongly influence the mode properties. We investigate the effect of the vertex angle α and the gap g on mode properties of

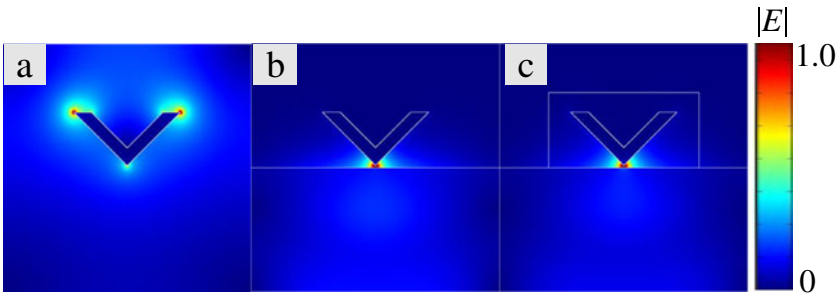

Fig. 2 Contour profiles of the normalized |E| fields of **a** the V-shaped silver nanowire, **b** the V-shaped silver nanowire embedded in air clading above Si substrate, and **c** the proposed HPW

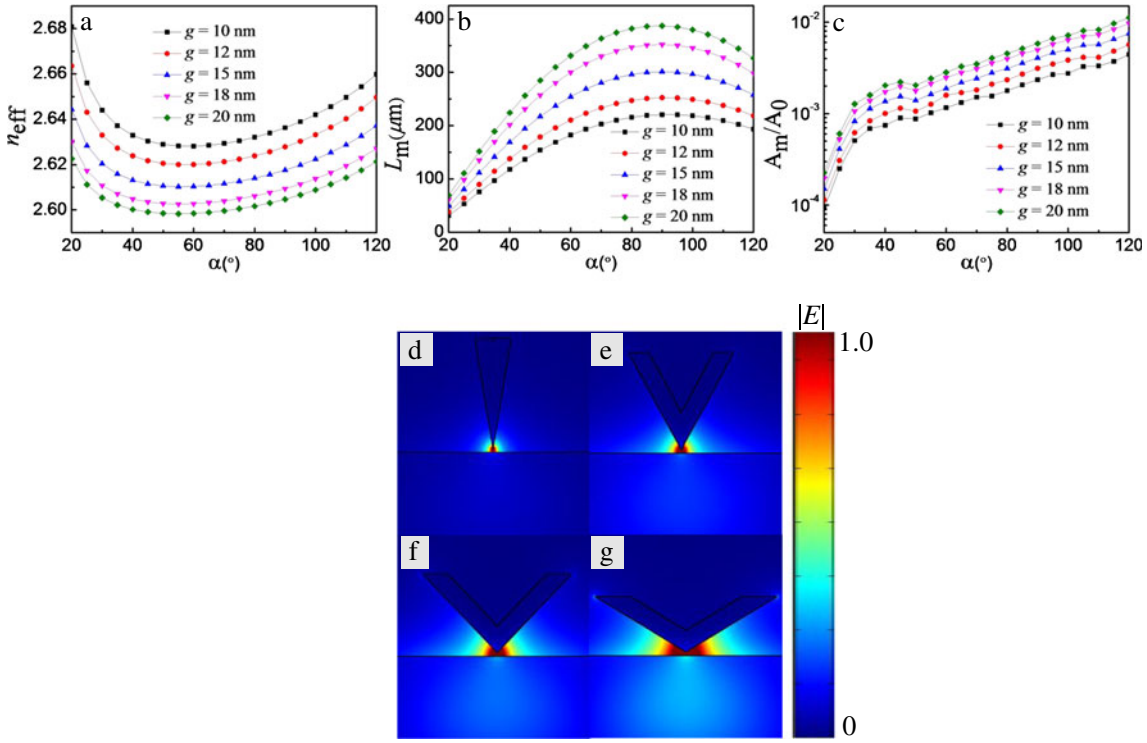

Fig. 3 Dependence of the V-haped HPW mode's properties on the vertex angle α with the different gap sizes g. **a** Real part of the mode effective index (n_{eff}). **b** the propagation length (L_m). **c** the normalized mode area (A_{eff}/A_0). Contour profiles of the normalized |E| fields of **d** [$\alpha = 20°$], **e** [$\alpha = 60°$], **f** [$\alpha = 90°$], and **g** [$\alpha = 120°$], with the gap size $g = 10$ nm

the V-shaped HPW, where the hypotenuse and thickness of the V-shaped silver wedge are fixed at 300 and 50 nm. Figure 3a–c shows the dependence of real part of the mode effective index (n_{eff}), the propagation length (L_m), and the normalized mode area (A_m/A_0), respectively, on the vertex angle α with the gap g. As shown in Fig. 3a–c, when the vertex angle α increases from 20 to 120°, the normalized mode area increasing monotonically. The mode effective index decreasing at first and then increasing, the minima of the mode effective index happens when the vertex angle α is 60°. The propagation length increasing first before decreasing, leading to a moderate angle α of 90°. From Fig. 3b, c, we can see that at the same vertex angle α, the propagation length and the normalized mode area increase by increasing the gap g.

To depict this phenomenon, we not only plot the electric field pattern, but also investigated the energy confinement ratio in the low-index cladding, metal and semiconductor substrate with change of α in the case of $g = 10$ nm, respectively. For a small vertex angle (less than 90°), as shown in Fig. 3d where the electric field is highly localized around the metal nanowedge tip,

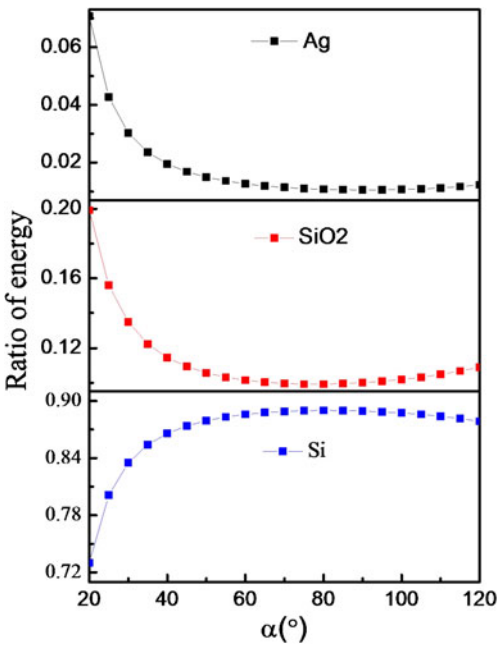

Fig. 4 Energy confinement ratio of the HPW with different angle α ($g = 10$ nm) in silver, cladding and semiconductor substrate regions, respectively

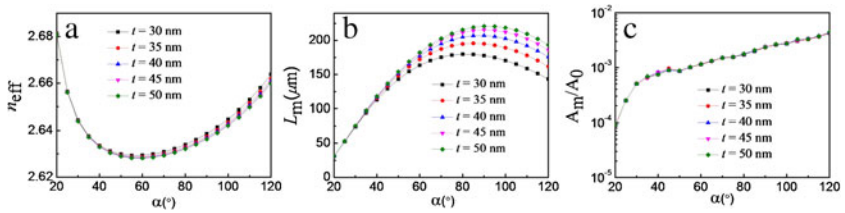

Fig. 5 Dependence of the V-shaped HPW mode's properties on the vertex angle α ($g = 10$ nm) with fixed $l = 300$ nm for different t. **a** Real part of the mode effective index (n_{eff}). **b** the propagation length (L_m). **c** the normalized mode area (A_{eff}/A_0)

which will result in a shorter propagation length due to relatively high ohmic loss. If the vertex angle is larger than 90°, a greater proportion of the electric field spreads laterally along the metal wedge, leading to a significantly increased mode area, resulting in a larger scattering loss and shorter propagation length.

In order to explain the behaviors of the n_{eff}, L_m, and A_m/A_0 more clearly, the energy confinement ratio was investigated, as shown in Fig. 4. The energy confinement ratio is defined as the ratio of the energy confined in certain area to the total energy. The loss of the HPW mainly depends on the absorption of the metal, the energy distributed in the metal region decreasing first before it increasing as shown in Fig. 4 leads to the propagation length increasing first before it decreasing (shown in Fig. 3b), for a appropriate vertex angle such as 90°, relatively less energy is distributed in the metal region resulting in a longer propagation length. Since the energy distributed in the silica cladding decreases at first and then increases as shown in Fig. 4, the interaction between the silicon substrate and the metal becomes weak at first and then strong, leading to a decrease at first and then an increase in n_{eff} (shown in Fig. 3a). For the A_m/A_0, its behavior is in accord with the analysis that field confinement is stronger in small vertex angle area α and vice versa.

Next, we investigate the effect of the vertex angle on the properties of the HPW with different V-shaped silver wedge thickness, the other parameters of the waveguide are fixed at $g = 10$ and $l = 300$ nm, as shown in Fig. 5a–c. For a small vertex angle α, the electric field is highly localized around the metal nanowedge tip, resulting in the n_{eff} and L_m remaining unchanged by increasing the thickness of V-shaped silver wedge. While increasing the thickness of V-shaped silver wedge with a large vertex angle α, the weaker interaction between the silicon substrate and metal, leading to a decrease in n_{eff} and an increase in L_m. For the A_m/A_0, its behavior is in accord with the previous analysis that field confinement is depend on the vertex angle α with the same gap g.

The effect of the vertex angle α on the properties of the HPW with different V-shaped silver wedge hypotenuse is investigated, the other parameters of the waveguide are fixed at $g = 10$ and, $t = 40$ nm, as shown in Fig. 6a–c. From Fig. 6, we can see that at a larger vertex angle α, the increased hypotenuse of V-shaped silver wedge could result in further reduced propagation loss, leading to a propagation length slightly increasing, while at a small vertex angle α, the n_{eff} and L_m can still be maintained unchanged. For the A_m/A_0, its behavior is dependent on the vertex angle α.

Conclusion

In this paper, we have proposed a V-shaped HPW which consists of a V-shaped silver nanowire embedded in a low-index dielectric cladding above a semiconductor substrate. The existence of a low-index dielectric nanoscale gap and sharp metallic edges could cause strong field enhancement in the nanoscale gap and thus enabling a strong confinement with reasonable propagation length. Our proposed structure is potential for building ultra-compact plasmonic devices and high-density photonic integrated circuits.

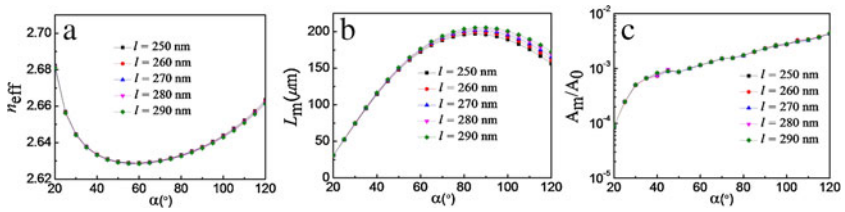

Fig. 6 Dependence of the V-shaped HPW mode's properties on the vertex angle α ($g = 10$ nm) with fixed $t = 40$ nm for different l. **a** Real part of the mode effective index (n_{eff}). **b** The propagation length (L_m). **c** The normalized mode area (A_{eff}/A_0)

Acknowledgments The work is financially supported by National Natural Foundation of China (Grant No. 61575117), the Fundamental Research Funds for the Central Universities of Ministry of Education of China (Grant No. GK201601008), and the Fostering Fund of Xian university of science and technology (Grant No. 2010045).

References

1. Raether H (1998) Surface plasmons. Springer, Berlin Heidelberg
2. Barnes WL, Dereux A, Ebbesen TW (2003) Surface plasmon subwavelength optics. Nature 424:824–830
3. Ozbay E (2006) Plasmonics: merging photonics and electronics at nanoscale dimensions. Science 311:189–193
4. Manjacavas A, Garcia de Abajo FJ (2009) Robust plasmon waveguides in strongly interacting nanowire array. Nano Lett 9:1285–1289
5. Zhang ZX, Hu ML, Chan KT, Wang CY (2009) Plasmonic waveguiding in a hexagonally ordered metal wire array. Opt Lett 35:3901–3903
6. Zou CL, Sun FW, Xiao YF, Dong CH, Chen XD, Cui JM, Gong Q, Han ZF, Guo GC (2010) Plasmon modes of silver nanowire on a silica substrate. Appl Phys Lett 97:183102
7. Bian YS, Gong QH (2013) Metallic nanowire-loaded plasmonic slot waveguide for highly confined light transport at telecom wavelength. IEEE J Quantum Electron 49:870–876
8. Veronis G, Fan SH (2005) Guided subwavelength plasmonic mode supported by a slot in a thin metal film. Opt Lett 30:3359–3361
9. Dionne JA, Swearlock LA, Atwater HA, Polman A (2006) Plasmon slot waveguides: towards chip-scale propagation with subwavelength-scale localization. Phys Rev B 73:035407
10. Ly-Gagnon DS, Kocabas SE, Miller DAB (2008) Characteristic impedance model for plasmonic metal slot waveguides. IEEE J Sel Topics Quantum Electron 14:1473–1478
11. Liu L, Han ZH, He SL (2005) Novel surface plasmon waveguide for high integration. Opt Exp 13:6645–6650
12. Han Z, Elezzabi AY, Van V (2010) Experimental realization of subwavelength plasmonic slot waveguides on a silicon platform. Opt Lett 35:502–504
13. Bozhevolnyi SI, Volkov VS, Devaux E, Ebbesen TW (2005) Channel plasmon-polariton guiding by subwavelength metal grooves. Phys Rev Lett 95:046802
14. Pile DFP, Gramotnev DK (2004) Channel plasmon-polariton in a triangular groove on a metal surface. Opt Lett 29:1069–1071
15. Maier SA, Friedman MD, Barclay PE, Painter O (2005) Experimental demonstration of accessible metal nanoparticle plasmon waveguides for planar energy guiding and sensing. Appl Phys Lett 86:071103
16. Fu YL, Hu XY, Lu CC, Yue S, Yang H, Gong QH (2012) All-optical logic gates based on nanoscale plasmonic slot waveguides. Nano Lett 12:5784–5790
17. Oulton RF, Sorger VJ, Zentgraf T, Ma RM, Gladden C, Dai L, Bartal G, Zhang X (2009) Plasmon lasers at deep subwavelength scale. Nature 461:629–632
18. Sorger VJ, Ye Z, Oulton RF, Wang Y, Bartal G, Yin X, Zhang X (2011) Experimental demonstration of low-loss optical waveguiding at deep sub-wavelength scales. Nature Commun 2:331
19. Oulton RF, Sorger VJ, Genov DA, Pile DFP, Zhang X (2008) A hybrid plasmonic waveguide for subwavelength confinement and long-range propagation. Nat Photon 2:496–500
20. Dai D, He S (2009) A silicon-based hybrid plasmonic waveguide with a metal cap for a nano-scale light confinement. Opt Exp 17:16646–16653
21. Fujii M, Leuthold J, Freude W (2009) Dispersion relation and loss of subwavelength confined mode of metal-dielectric-gap optical waveguides. IEEE Photon Technol Lett 21:362–364
22. Su Y, Zheng Z, Bian Y, Liu Y, Liu J, Zhu J, Zhou T (2011) Low-loss silicon-based hybrid plasmonic waveguide with an air nano trench for sub-wavelength mode confinement. Micro Nano Lett IET 6:643–645
23. Lou F, Dai DX, Wosinski L (2012) Ultracompact polarization beam splitter based on a dielectric–hybrid plasmonic–dielectric coupler. Opt Lett 37:3372–3374
24. Volkov VS, Han ZH, Nielsen MG, Leosson K, Keshmiri H, Gosciniak J, Albrektsen O, Bozhevolnyi SI (2011) Long-range dielectric-loaded surface plasmon polariton waveguides operating at telecommunication wavelengths. Opt Lett 36:4278–4280
25. Ma YQ, Farrell G, Semenova Y, Wu Q (2014) Hybrid nanowedge plasmonic waveguide for low loss propagation with ultra-deep-subwavelength mode confinement. Opt Lett 39:973–976
26. Bian YS, Gong QH (2014) Long-range hybrid ridge and trench plasmonic waveguides. Appl Phys Lett 104:251115
27. Olyaeefar B, Khoshsima H (2014) Low-loss ultra-subwavelength hybrid plasmonic waveguide based on metallic bump structures. J Phys D Appl Phys 47:105105
28. Wijesinghe T, Premaratne M, Agrawal GP (2014) Electrically pumped hybrid plasmonic waveguide. Opt Exp 22:2681–2694
29. Amirhosseini A, Safian R (2013) A Hybrid plasmonic waveguide for the propagation of surface plasmon polariton at 1.55μm on SOI substrate. IEEE Trans Nanotechnol 12:1031–1036
30. Xiang C, Wang J (2013) Long-range hybrid plasmonic slot waveguide. IEEE Photon J 5:4800311
31. Zhang T, Chen L, Li X (2013) Reduction of propagation loss by introducing hybrid plasmonic model in graded-grating based "trapped rainbow" system. Opt Commun 301–302:116–120
32. Mu JW, Chen L, Li X, Huang WP, Kimerling LC, Michel J (2013) Hybrid nano ridge plasmonic polaritons waveguides. Appl Phys Lett 103:131107
33. Alam MZ, Bahrami F, Aitchison JS, Mojahedi M (2014) Analysis and optimization of hybrid plasmonic waveguide as a platform for biosensing. IEEE Photon J 6:3700110
34. Tian JP, Zhang CJ, Liang XJ, Li HJ (2013) Mode analysis of a symmetric hybrid surface plasmonic waveguide for photonic integration. IEEE Photon Technol Lett 49:331–334
35. Pile DFP, Gramotnev DK (2005) Plasmonic subwavelength waveguides: next to zero losses at sharpbends. Opt Lett 30:1186–1188
36. Johnson PB, Christy RW (1972) Optical constants of the noble metals. Phys Rev B 6:4370–4379